



TUMORIGENESIS AND NEOPLASTIC PROGRESSION

36-kDa Annexin A3 Isoform Negatively Modulates Lipid Storage in Clear Cell Renal Cell Carcinoma Cells



Silvia Bombelli,^{*} Barbara Torsello,^{*} Sofia De Marco,^{*} Giuseppe Lucarelli,[†] Ingrid Cifola,[‡] Chiara Grasselli,^{*} Guido Strada,[§] Giorgio Bovo,[¶] Roberto A. Perego,^{*} and Cristina Bianchi^{*}

From the School of Medicine and Surgery,^{*} University of Milano-Bicocca, Monza; the Department of Emergency and Organ Transplantation-Urology,[†] University of Bari, Bari; the Institute for Biomedical Technologies,[‡] National Research Council, Segrate; the Urology Unit,[§] ASST North Milan, Bassini Hospital, Cinisello Balsamo; and the Pathology Unit,[¶] ASST North Milan, Vimercate Hospital, Vimercate, Italy

Accepted for publication
August 18, 2020.

Address correspondence to
Cristina Bianchi, Ph.D., or
Roberto A. Perego, M.D.,
School of Medicine and Sur-
gery, Via Cadore 48, Monza
20900, Italy. E-mail: cristina.bianchi@unimib.it or roberto.perego@unimib.it.

The adipocyte-like morphology of clear cell renal cell carcinoma (ccRCC) cells results from a grade-dependent neutral lipid accumulation; however, the molecular mechanism and role in renal cancer progression have yet to be clarified. ccRCC shows a gene expression signature consistent with adipogenesis, and the phospholipid-binding protein annexin A3 (AnxA3), a negative regulator of adipocyte differentiation, is down-regulated in RCC and shows a differential expression pattern for two isoforms of 36 and 33 kDa. Using primary cell cultures and cell lines, we investigated the involvement of AnxA3 isoforms in lipid storage modulation of ccRCC cells. We found that the increased accumulation of lipids into ccRCC cells correlated with a decrease of the 36/33 isoform ratio. Treatment with adipogenic medium induced a significant increment of lipid storage in ccRCC cells that had a low 36-kDa AnxA3 expression and 36/33 ratio. The 36-kDa AnxA3 silencing in ccRCC cells increased lipid storage induced by adipogenic medium. These data suggest that 36-kDa AnxA3 negatively modulates the response to adipogenic treatment and may act as negative regulator of lipid storage in ccRCC cells. The subcellular distribution of AnxA3 in the cellular endocytic compartment suggests its involvement in modulation of vesicular trafficking, and it might serve as a putative mechanism of lipid storage regulation in ccRCC cells, opening novel translational outcomes. (*Am J Pathol* 2020, 190: 2317–2326; <https://doi.org/10.1016/j.ajpath.2020.08.008>)

The most striking phenotypic characteristic of clear cell renal cell carcinoma (ccRCC) is the morphology of its clear cells, which resemble adipocytes as a result of neutral lipid accumulation¹ that has been observed to be a grade-dependent phenomenon.² The molecular mechanism behind this clear cell morphology has yet to be clarified to shed light on renal cancer progression. Among the different putative mechanisms involved in the storage of neutral lipids inside the ccRCC cells, the increased uptake of exogenous lipids mediated by a hypoxia-inducible factor (HIF) 1–dependent up-regulation of the very-low-density lipoprotein receptor may also be important.^{3,4} The increased uptake of exogenous lipids is involved in the formation of lipid droplets even in adipocytes.⁵ In addition,

ccRCC tissue samples show a gene expression signature consistent with adipogenesis, and ccRCC cells can undergo adipogenic transdifferentiation after specific treatment.⁶ More recently, the annexin A3 (AnxA3) protein has been described to play an important role as a negative regulator of

Supported by Fondo d'Ateneo per la Ricerca of Milano-Bicocca University grants 2016-ATE-0273 (C.B.) and 2017-ATE-0252 (C.B.) and by Associazione Gianluca Strada Onlus (AGS) grant 2017-CONT- 0070 (R.A.P.). S.B. was recipient of a Postdoctoral Fellowship and S.D.M. and C.G. were recipients of Ph.D. Fellowships from Ministero Istruzione, Università e Ricerca.

S.B., B.T., and S.D.M. contributed equally to this work as first authors. R.A.P. and C.B. contributed equally to this work as senior authors. Disclosures: None declared.

adipocyte differentiation in adipose tissue.⁷ AnxA3 was highly expressed in pre-adipocytes and down-regulated at an early phase of adipocyte differentiation. Notably, a decrease of AnxA3 was required to prime the adipocyte differentiation. AnxA3 belongs to the annexin family of Ca²⁺-dependent phospholipid-binding proteins⁸ and shows the ability to enhance angiogenesis,⁹ plays pivotal roles in promoting growth and stem cell-like features in hepatocellular carcinoma cells,¹⁰ and is overexpressed in ovarian cancer, in which it may serve as biomarker for platinum resistance.^{11,12} Conversely, a down-regulation of AnxA3 is described in prostate cancer¹³ and in renal cell carcinoma,¹⁴ where two AnxA3 isoforms of 36 and 33 kDa, which originate as a result of an alternative splicing event, have been previously highlighted. These two isoforms showed a differential expression pattern in RCC and normal renal tubular cells; in particular, the 36-kDa isoform is more abundant in normal cells, whereas the 33-kDa isoform is up-regulated in RCC cells.

On the basis of these findings, in this study, we have investigated the involvement of AnxA3 isoforms in the lipid storage process, which characterizes the clear cell adipocyte-like morphology of ccRCC cells. Normal tubular and ccRCC primary cell cultures and cell lines were instrumental for this purpose.

Materials and Methods

Primary Cell Cultures

Primary cell cultures were obtained from normal cortex ($n = 28$) and tumor ($n = 44$) tissue specimens of 44 ccRCC patients (30 men and 14 women; median age, 69 years) following nephrectomy. The collected tissues were those exceeding the diagnostic needs. The normal cortex was taken from a healthy region of the kidney without any indication of cancer. All procedures were performed after written consent and were approved by the Local Ethical Committee. Tumors were classified as 22 pT1, 7 pT2, and 10 pT3 and as 3 grade 1, 26 grade 2, 14 grade 3, and 1 grade 4, according to World Health Organization/International Society of Urologic Pathologists grading system.

The culture conditions and immunophenotypic characterization were performed as described.¹⁴ The primary cell cultures were used at the first confluence.

TCGA ccRCC Tissue Data Set Analysis

Expression of 36-kDa AnxA3 isoform and perilipin-2 (PLIN2) was validated at transcript level in The Cancer Genome Atlas (TCGA, <http://portal.gdc.cancer.gov>, last accessed September 08, 2020) Kidney Renal Clear Cell Carcinoma (KIRC) data set, using the RNA-sequencing profiling data available in Gene Expression Profiling Interactive Analysis webtool¹⁵ for 523 ccRCC tissue cases and 100 normal cortex tissue cases (72 from TCGA KIRC data

set and 28 from Genotype Tissue Expression portal). Normalized read counts are expressed as transcripts per million.

Cell Lines and Adipogenic Medium

Human proximal tubular (HK2) and ccRCC (A498 and Caki1) cell lines were obtained from ATCC (Manassas, VA). HK2 cells were cultured in Dulbecco's modified Eagle's medium—F12 (Lonza, Basel, Switzerland) containing 5% fetal bovine serum, 5 µg/mL insulin, 5 µg/mL transferrin, 5 ng/mL sodium selenite, 36 ng/mL hydrocortisone, 40 pg/mL triiodothyronine, 5 pg/mL prostaglandin E (Sigma, St. Louis, MO), and 10 ng/mL epidermal growth factor (Cell Signaling Technology, Danvers, MA). A498 (*VHL*^{-/-}; HIF1a-negative and HIF2a-positive) and Caki1 (*VHL* wild type; HIF1a- and HIF2a-positive) cells¹⁶ were cultured in Dulbecco's modified Eagle's medium (Euroclone, Milan, Italy) with 10% fetal calf serum. Both media were supplemented with 1% penicillin/streptomycin and 1% amphotericin B (Euroclone).

To induce lipid storage, the different cell lines were grown for 8 days in an adipogenic medium composed of complete culture media supplemented with 0.1 µmol/L dexamethasone, 10 µg/mL insulin, 100 µmol/L indomethacin, and 500 µmol/L isobutylmethylxanthine (Sigma).

Hematoxylin-Eosin and Oil Red O Staining

Hematoxylin-eosin staining was performed on formalin-fixed, paraffin-embedded tissue sections following standard protocols¹⁷ and corresponding images were kindly provided by Francesca Sanguedolce (University of Foggia, Foggia, Italy). Oil Red O staining was performed on formalin-fixed cells, as described.¹⁸ The stained samples were analyzed by Nikon Eclipse E800 microscope with 20× objectives (Nikon Instruments, Firenze, Italy), and the corresponding images were captured and analyzed by a LuciaG Image analysis system (Nikon Instruments).

Cell Fractionation, Protein Extraction, and Western Blot Analysis

First-confluent primary cell cultures and cell lines were lysed to obtain total homogenate and nuclear and nuclear-free fractions, as previously described.¹⁹ A membrane fraction was also obtained from primary cell cultures, as described.²⁰ Protein lysates (30 µg), quantified using a bicinchoninic acid microassay (Sigma-Aldrich, St. Louis, MO) and separated on NuPage 4% to 12% Bis-Tris precast gels (Thermo Fisher, Waltham, MA),²¹ were submitted to Western blotting²² with mouse monoclonal antibodies against PLIN2 (dilution 1:500; AP125; Progen, Heidelberg, Germany) and HIF1α (dilution 1:500; 54; BD Biosciences, San José, CA) and with rabbit polyclonal antibodies against AnxA3 (1.25 µg/mL; ab33068; Abcam, Cambridge, MA),

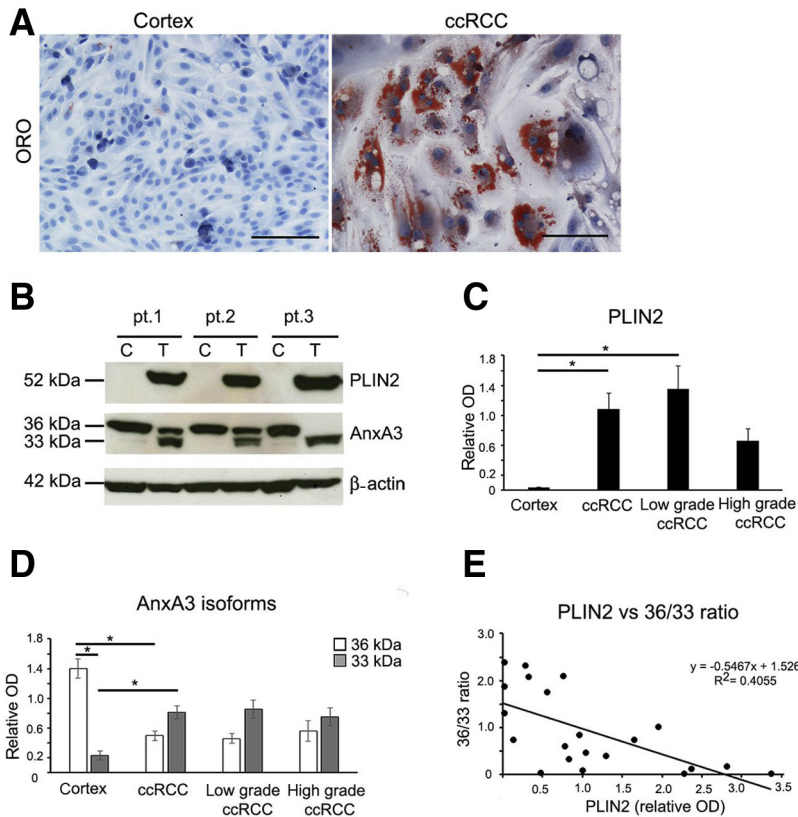


Figure 1 Lipid storage and annexin A3 (AnxA3) isoform pattern in normal cortex and clear cell renal cell carcinoma (ccRCC) primary cell cultures. **A:** Representative images of normal cortex and ccRCC primary cell cultures captured after Oil Red O (ORO) staining. **B:** Representative Western blot analysis of perilipin-2 (PLIN2) and AnxA3 isoforms performed in total homogenates of matched cortex (C) and ccRCC (T) primary cultures established from three different patients. **C:** Densitometric analysis of PLIN2 protein bands detected in total homogenates of 10 cortex and 21 ccRCC (13 low-grade and 8 high-grade) primary cultures and normalized for β -actin bands. **D:** Densitometric analysis of the 36- and 33-kDa AnxA3 bands detected in total homogenates of 18 cortex and 36 ccRCC (22 low-grade and 14 high-grade) primary cultures and normalized for β -actin bands. **E:** Linear regression analysis between PLIN2 expression and the quantitative ratio between 36- and 33-kDa AnxA3 isoforms (36/33 ratio) evaluated by Western blot analysis in 21 ccRCC primary culture total homogenates. **Solid black line** represents the line of regression. Data are expressed as means \pm SEM (**C** and **D**). * $P < 0.05$ (one-way analysis of variance analysis with post-hoc Tukey corrected t -test). Scale bars = 100 μ m (**A**). Original magnification, $\times 200$ (**A**). pt., patient.

Na^+/K^+ ATPase α -1 (dilution 1:1000; Millipore, Burlington, MA), α -tubulin (10 μ g/mL; Molecular Probes Invitrogen, Carlsberg, CA), acetyl-histone H3 (10 μ g/mL; Upstate Biotechnology, Lake Placid, NY), and β -actin (dilution 1:1000; Sigma-Aldrich). Densitometric analysis of specific bands was performed by ImageJ software version 1.48v (NIH, Bethesda, MD; <http://imagej.nih.gov/ij>), and specific band intensities were normalized for corresponding β -actin band.

Cell Viability Assay

Cell viability was evaluated using the FITC Annexin V Apoptosis detection kit and propidium iodide (Biolegend, San Diego, CA), according to the manufacturer's instructions, as previously described.² Fluorescence-activated cell sorting (FACS) analysis was performed on 10,000 events with a MoFlo Astrios Cell Sorter equipped with Summit software version 6.1 (Beckman Coulter, Milano, Italy). The offline analysis was performed using Kaluza software version 1.2 (Beckman Coulter, Brae, CA). Viable cells (annexin V and propidium iodide negative) were expressed as a percentage with respect to the total events analyzed.

Bodipy Staining and FACS Analysis

Live cells were washed twice in phosphate-buffered saline and incubated with the fluorescent neutral lipid dye Bodipy

493/503 (5 μ g/mL; Thermo Fisher) for 15 minutes at room temperature. After staining, cells were washed twice in phosphate-buffered saline and fixed in 4% paraformaldehyde for 10 minutes. Fixed cells were washed in phosphate-buffered saline, and FACS analysis was performed on 10,000 events with a MoFlo Astrios Cell Sorter, using Summit 6.1 and Kaluza software version 1.2 (Beckman Coulter, Brae, CA). Mean Bodipy fluorescence intensity of the cells grown in adipogenic medium was expressed as a percentage with respect to the cells grown in control medium (100%).

Immunocytofluorescence

Cells grown on glass coverslips were fixed in 4% paraformaldehyde, incubated with mouse monoclonal anti-PLIN2 (dilution 1:50; AP125; Progen), anti-early endosome antigen 1 (1:500; BD Biosciences), anti-130 kDa cis-Golgi matrix protein (1:700; BD Biosciences), or rabbit polyclonal anti-AnxA3 (1:50; Abcam) primary antibodies and Alexa Fluor 488 or 594 conjugated anti-mouse or anti-rabbit secondary antibodies (dilution 1:100; Invitrogen), as previously described.¹⁷ Those cells fixed and stained with the fluorescent antibodies were finally treated with 5 μ g/mL Bodipy for 30 minutes at room temperature to indicate lipid droplets. Those cells grown on coverslips were treated with 100 nmol/L Mitotracker Red CMXRos (Molecular Probes Invitrogen) in culture medium for 30 minutes at 37°C and

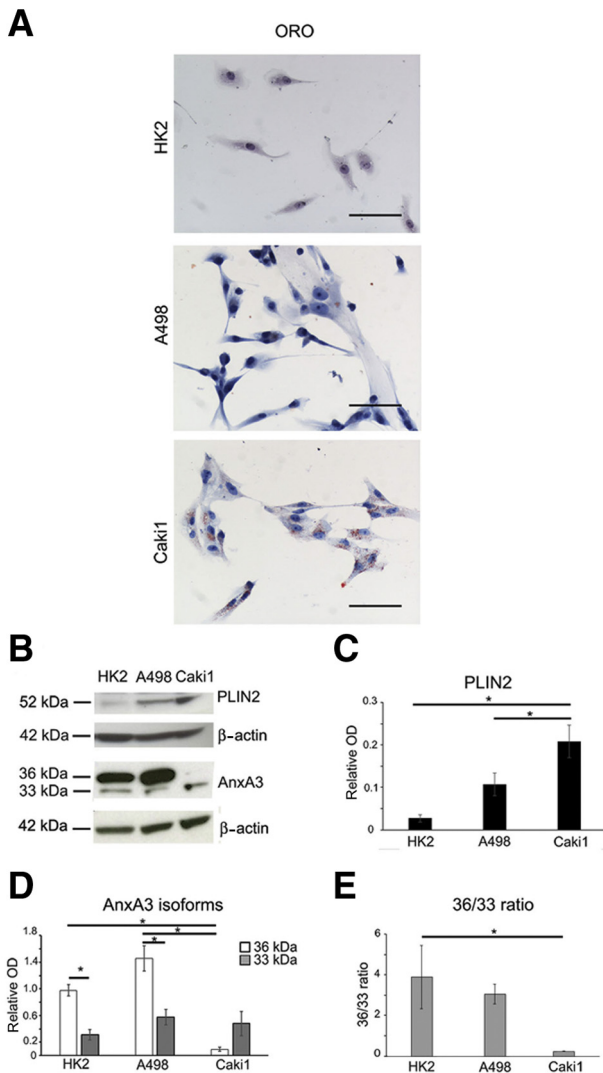


Figure 2 Lipid storage and annexin A3 (AnxA3) isoform pattern in normal cortex and clear cell renal cell carcinoma (ccRCC) cell lines. **A:** Representative images of normal cortex (HK2) and ccRCC (A498 and Caki1) cell lines captured after Oil Red O (ORO) staining. **B:** Representative Western blot analysis of perilipin-2 (PLIN2) and AnxA3 isoforms performed in total homogenates of HK2, A498, and Caki1 cell lines. β -Actin bands assessed loading. **C:** Densitometric analysis of PLIN2 protein bands detected in HK2, A498, and Caki1 cell line total homogenates and normalized for β -actin bands. **D:** Densitometric analysis of the 36- and 33-kDa AnxA3 bands detected in HK2, A498, and Caki1 cell line total homogenates and normalized for β -actin bands. **E:** Densitometric ratio between 36- and 33-kDa AnxA3 bands (36/33 ratio) in HK2, A498, and Caki1 total homogenates. Data are expressed as means \pm SEM of at least three independent experiments (C–E). * $P < 0.05$ (one-way analysis of variance analysis with post-hoc Tukey corrected t -test). Scale bars = 100 μ m (A). Original magnification, $\times 200$ (A).

fixed with 4% paraformaldehyde for 15 minutes at 37°C. Nuclear counterstaining was obtained with DAPI (Sigma). Coverslips were mounted onto glass slides with CC/mount (Sigma). Immunofluorescence images were obtained with a Zeiss LSM710 confocal microscope equipped with Zen2009 software 2009 (Zeiss, Oberkochen, Germany), using 40 \times or 63 \times objective (Zeiss).

36-kDa AnxA3 Isoform and PLIN2 Knockdown

A total of 1.5×10^5 A498 and Caki1 cells, grown for 12 hours in complete culture medium, were respectively transfected, as previously described,¹⁹ with siRNA 5'-CAGAAAGCAAUCAGAGGAA-3' targeting the exon III of the human AnxA3 (*ANXA3*) gene¹⁴ for specific silencing of the 36-kDa isoform, and with ON-TARGETplus human *PLIN2* SMART pool siRNA (Thermo Scientific Dharmacon, Lafayette, CO). Both cell lines were transfected also with ON-TARGETplus Control pool siRNA (Thermo Scientific Dharmacon) and cultured for 96 hours in control or adipogenic medium.

Statistical Analysis

Data, expressed as means \pm SEM, were analyzed using paired t -test (for single comparison of treated samples versus controls) or one-way analysis of variance analysis with the post-hoc Tukey corrected t -test (for multiple group comparisons) performed with Origin software version 93E (Originlab, Northampton, MA). Correlation analyses were performed by computing the Pearson or Spearman correlation coefficient (r) and linear regression analysis²³ with Origin software. $P < 0.05$ was considered as statistically significant.

Results

Lipid Storage and AnxA3 Isoform Expression Pattern in ccRCC Cells

The normal cortex and ccRCC primary cell cultures were characterized for intracellular lipid storage by Oil Red O staining (Figure 1A) and Western blot analysis of PLIN2 (Figure 1B), the lipid droplet coat protein described as a marker of intracellular neutral lipid storage in nonadipose tissues.²⁴ In accordance with previous data,² PLIN2 protein was significantly more abundant in ccRCC than in normal cortex cultures (Figure 1C). Moreover, its expression was higher in low-grade (grade 1 to grade 2) with respect to high grade (grade 3 to grade 4) ccRCC samples (Figure 1C), and this difference was significant ($P = 0.030$) if evaluated by t -test. The difference in lipid droplet content between low- and high-grade samples was morphologically evident also in corresponding hematoxylin-eosin stained ccRCC tissues (Supplemental Figure S1A). The protein expression of AnxA3 isoforms (36 and 33 kDa) was also evaluated in the primary cultures by Western blot analysis (Figure 1B), confirming data previously obtained in a different population of RCC patients.¹⁴ In particular, the 36-kDa isoform was significantly down-regulated in ccRCC cultures with respect to cortex cultures. The 36-kDa isoform was also down-regulated with respect to the 33-kDa isoform in ccRCC cultures, but significantly up-regulated in cortex cultures. Instead, the 33-kDa isoform was significantly

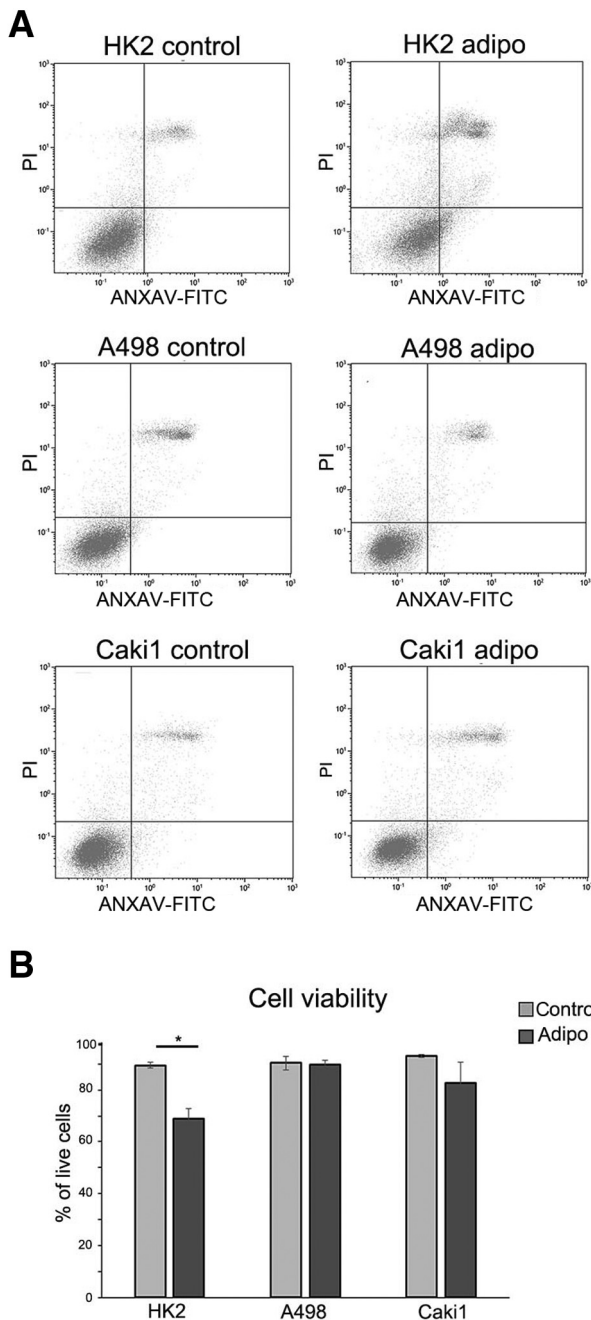


Figure 3 Viability of normal cortex and clear cell renal cell carcinoma (ccRCC) cell lines after adipogenic treatment. **A:** Representative images of fluorescence-activated cell sorting (FACS) analysis performed with annexin V (ANXAV)/propidium iodide (PI) in HK2, A498, and Caki1 cell lines cultured for 8 days in normal culture medium (control) or in adipogenic medium (adipo). **B:** Quantification of viable cells after 8 days of culture in control or adipogenic medium, expressed as percentage of annexin V and PI negative cells (bottom left quadrant of each plot shown in **A**) with respect to total events analyzed (100%). Data are given as means \pm SEM of three independent experiments (**B**). * $P < 0.05$ (paired t -test). FITC, fluorescein isothiocyanate.

incremented in ccRCC cultures with respect to cortex cultures (Figure 1D). Therefore, in ccRCC, the quantitative ratio between the 36- and 33-kDa isoforms was lower than 1 (0.88 ± 0.14) and inverted with respect to cortex cultures

(15.99 ± 6.56). Notably, this 36/33 ratio was lower in low-grade ccRCC cultures, which showed more abundant lipid storage, than in high-grade cultures (0.82 ± 0.14 versus 0.98 ± 0.28), although this difference was not statistically significant ($P = 0.57$) (Figure 1, C and D). Moreover, PLIN2 protein expression was significantly higher (Supplemental Figure S1B) and 36/33 ratio lower (Supplemental Figure S1C) in HIF1 α -positive than in HIF1 α -negative ccRCC primary cultures.

In agreement with these results, a significant reduced expression of the transcript coding for 36-kDa AnxA3 isoform and increased expression of PLIN2 transcript were found in TCGA KIRC tissue cases compared with normal cortex tissue cases (Supplemental Figure S1D).

Because variability in lipid storage was evident among the different ccRCC samples, it was investigated whether PLIN2 expression (used as lipid storage marker) correlated with the AnxA3 isoform pattern, expressed as a 36/33 ratio, and a significant negative correlation (Pearson coefficient $r = -0.64$; $P = 0.002$) was found, as shown by linear regression analysis (Figure 1E). A significant negative correlation (Pearson coefficient $r = -0.47$; $P = 0.031$) was found even between PLIN2 and 36-kDa AnxA3 isoform protein expression (Supplemental Figure S1E). Notably, Spearman correlation test performed on the TCGA KIRC tissue data set showed an inverse correlation between *PLIN2* and *36-kDa ANXA3* mRNA expression as well ($r = -0.10$; $P = 0.018$) (Supplemental Figure S1F).

The relation between lipid storage and the AnxA3 isoform pattern was investigated even in normal tubular (HK2) and ccRCC (A498 and Caki1) cell lines. As shown by Oil Red O staining (Figure 2A) and confirmed by analysis of PLIN2 protein expression (Figure 2, B and C), lipid storage was significantly more abundant into Caki1 cells, which showed a significant down-regulation of the 36-kDa AnxA3 isoform with respect to A498 and HK2 cells (Figure 2, B and D). Because of the low expression of 36-kDa AnxA3, the 36/33 ratio in Caki1 cells (0.22 ± 0.03) was inverted with respect to HK2 and A498 cells, in which it was >1 (Figure 2E). The increased lipid storage matched with the decrease of 36/33 ratio even in cell lines (Figure 2, C and E), confirming the relation between lipid storage and the AnxA3 isoform pattern observed in ccRCC primary cultures.

Lipid Storage and AnxA3 Isoform Expression Pattern in ccRCC Cell Lines after Adipogenic Treatment

To further characterize the relation between lipid storage and the AnxA3 isoform expression pattern, the ccRCC (A498 and Caki1) and normal tubular (HK2) cells were grown for 8 days in adipogenic medium to induce lipid storage. As shown by FACS analysis (Figure 3A), the adipogenic treatment significantly affected the viability (annexin V/propidium iodide-negative cells in bottom left quadrant of each plot) of HK2 cells only (Figure 3B). For

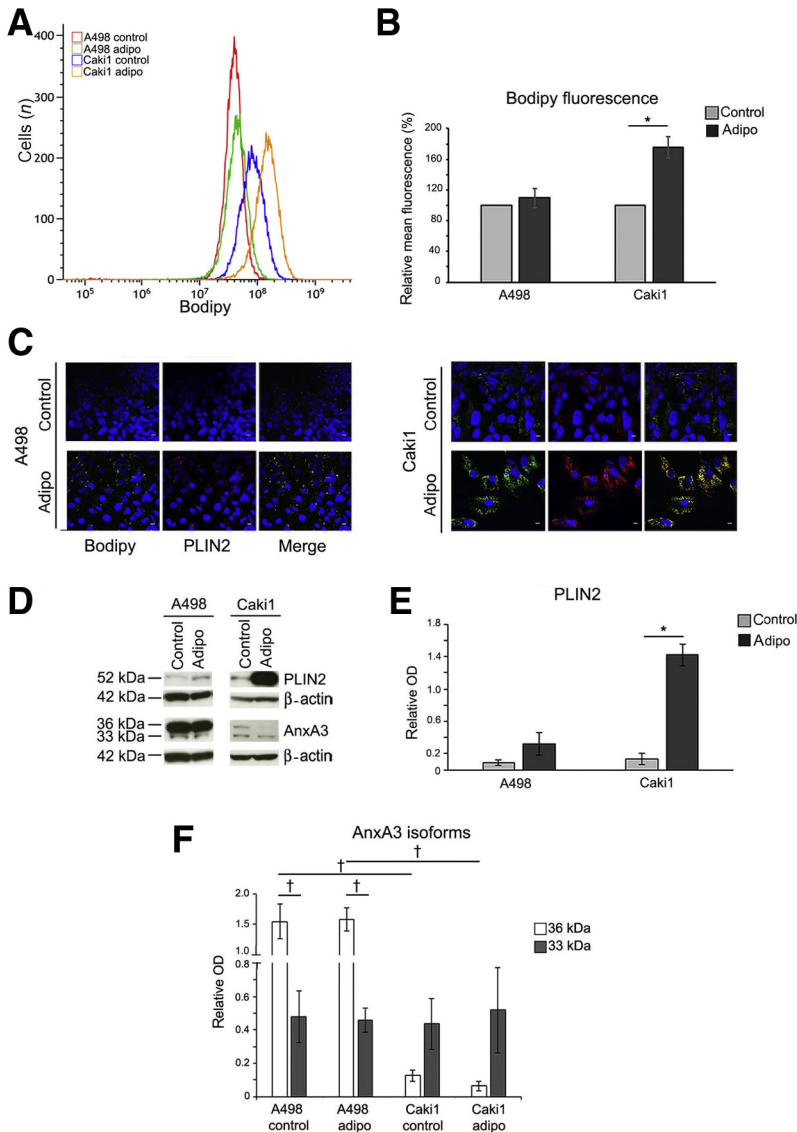


Figure 4 Effect of 8 days of adipogenic treatment (adipo) on lipid storage and annexin A3 (AnxA3) isoform pattern of clear cell renal cell carcinoma (ccRCC) cell lines. **A:** Representative fluorescence-activated cell sorting (FACS) analysis of Bodipy fluorescence performed in A498 and Caki1 treated cells. **B:** Quantification by FACS of Bodipy mean fluorescence intensity in A498 and Caki1 treated cells. Data expressed as percentage with respect to cells cultured in control medium (100%). At least three independent experiments were performed. **C:** Representative immunofluorescence images of A498 and Caki1 treated cells stained with Bodipy (green) and anti-perilipin-2 (PLIN2) antibodies (red). Colocalization signals (yellow) are shown in merge panels. DAPI was used to counterstain the nuclei in blue. **D:** Representative Western blot analysis of PLIN2 and AnxA3 isoform proteins performed in total homogenates of A498 and Caki1 treated cells. β -Actin bands assessed loading. **E:** Densitometric analysis of PLIN2 protein bands detected in total homogenates of A498 and Caki1 treated cells and normalized for β actin band. Four independent experiments were performed. **F:** Densitometric analysis of 36- and 33-kDa AnxA3 bands detected in total homogenates of A498 and Caki1 treated cells and normalized for β actin bands. Four independent experiments were performed. Data are expressed as means \pm SEM (**B**, **E**, and **F**). * $P < 0.05$ (paired t -test); $^{\dagger}P < 0.05$ (one-way analysis of variance analysis with post-hoc Tukey corrected t -test). Scale bar = 10 μ m (**C**). PLIN2, perilipin 2.

this reason, this cell line was not studied further. Conversely, after 8 days of treatment, A498 and Caki1 cells were stained with the lipid dye Bodipy 493/503 and analyzed by FACS (Figure 4A), which revealed a significant increase of lipid storage in treated Caki1 but not in A498 cells with respect to corresponding cells grown in control medium (Figure 4B). These data were confirmed even by PLIN2 immunofluorescence analysis performed in Bodipy-stained A498 and Caki1 cells grown in control and adipogenic media (Figure 4C), and by PLIN2 Western blot performed in the corresponding total homogenates (Figure 4D). Notably, in Caki1 cells, the significant increase of lipid storage observed after 8 days of adipogenic treatment (Figure 4E) matched with a further, although not significant, decrease of 36-kDa AnxA3 (Figure 4, D and F) and of 36/33 ratio from 0.22 to 0.14. Conversely, in A498 cells, 8 days of adipogenic treatment neither significantly increased the lipid

storage nor changed 36- and 33-kDa AnxA3 isoform expression (Figure 4, D–F). These data suggest that the overexpression of the 36-kDa AnxA3 isoform prevented a significant increment of lipid storage in A498 cells after 8 days of adipogenic treatment.

36-kDa AnxA3 Knockdown in A498 Cells Enhances the Lipid Storage Induced by Adipogenic Treatment

To prove that the 36-kDa AnxA3 acts as a negative regulator of lipid storage in ccRCC cells, its expression was specifically downregulated by siRNA in A498 cells in the presence of control or adipogenic medium. The 36-kDa AnxA3 protein level in A498 cells was 30% with respect to control cells after 96 hours of specific silencing in adipogenic medium (Figure 5, A and B). The silencing of 36-kDa AnxA3 isoform did not significantly affect the 33-kDa

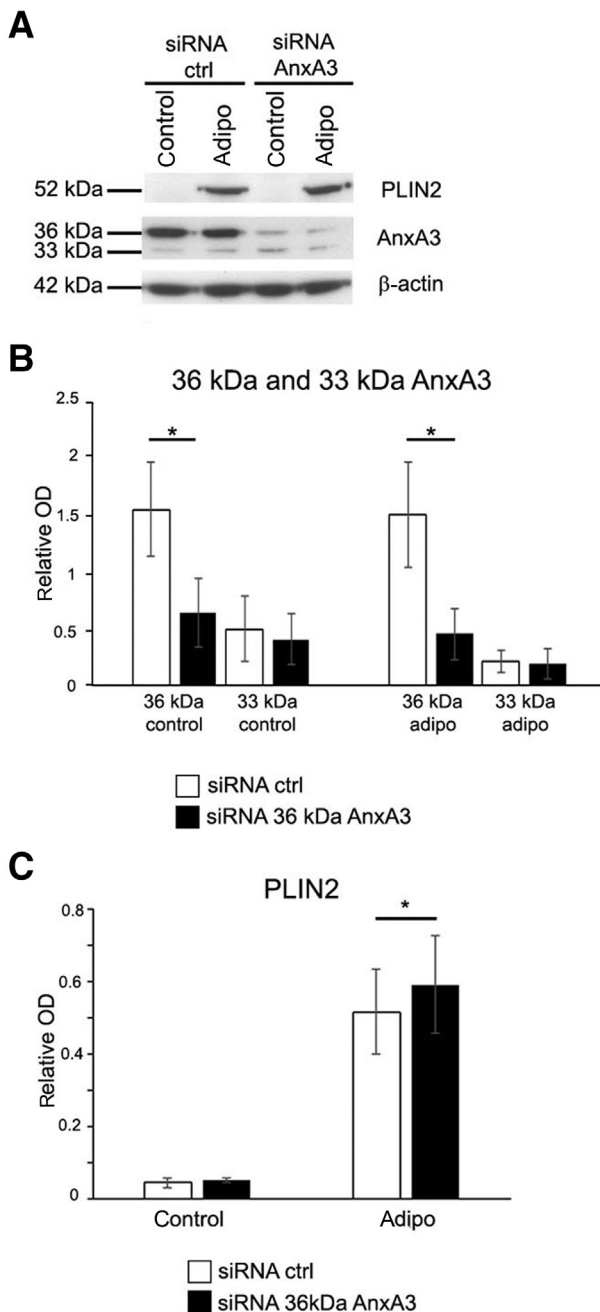


Figure 5 Effect of 36-kDa annexin A3 (AnxA3) silencing (siRNA AnxA3, alias siRNA *ANXA3*) on lipid storage of A498 cells cultured for 96 hours in adipogenic medium (adipo). **A:** Representative Western blot analysis of perilipin-2 (PLIN2) and AnxA3 isoforms performed in total homogenates of A498 treated cells. β -Actin bands assessed loading. **B:** Densitometric analysis of 36- and 33-kDa AnxA3 protein bands detected in total homogenates of A498 treated cells and normalized for β -actin bands. **C:** Densitometric analysis of PLIN2 protein bands detected in total homogenates of A498 treated cells and normalized for β -actin bands. Data expressed as means \pm SEM of three independent experiments (**B** and **C**). * $P < 0.05$ (paired *t*-test). Ctrl, control.

isoform expression (Figure 5, A and B) with consequent decrease of 36/33 ratio. After 96 hours of adipogenic treatment, 36-kDa AnxA3 knocked-down A498 cells showed a significant increment of PLIN2 protein expression

with respect to control siRNA-treated cells (Figure 5, A and C). PLIN2 silencing in Caki1 cells cultured for 96 hours in control or adipogenic medium did not affect AnxA3 isoform expression (Supplemental Figure S1G), suggesting that the modulation of AnxA3 isoform expression is PLIN2 independent. These data suggest that the down-regulation of 36-kDa AnxA3 and of 36/33 ratio enhances the lipid storage of ccRCC cells in response to adipogenic treatment.

Subcellular Distribution of AnxA3 Isoforms

To shed light on the mechanism by which AnxA3 modulates lipid storage in ccRCC cells, its subcellular distribution in normal cortex and ccRCC primary cultures was analyzed. As shown by Western blot analysis, the characteristic differential pattern of the two AnxA3 isoforms observed in total homogenates of cortex and ccRCC cells (Figure 1B) was maintained in corresponding purified nuclear-free fractions (Figure 6A). The 36-kDa isoform was detectable even in the purified nuclear fraction of normal cortex cells, and the well-known phospholipid-binding property of AnxA3 accounted for the bands of 36 and 33 kDa that were observed in the purified membrane fraction of both cortex and ccRCC cells (Figure 6A).

The distribution of AnxA3 in different membranous subcellular structures of primary normal cortex and ccRCC cells was also evaluated by immunofluorescence. The AnxA3 signal, detected with an antibody that recognized both isoforms, colocalized neither with mitochondrial structures, stained with Mitotracker, nor with the *cis*-Golgi marker 130 kDa *cis*-Golgi matrix protein (Figure 6B). Moreover, the AnxA3 signal did not colocalize with the lipid droplets visualized by Bodipy staining in ccRCC cells (Figure 6B). Instead, a yellow colocalization signal between AnxA3 and the early endosome marker early endosome antigen 1 was detected in both cortex and ccRCC cells (Figure 6B). The subcellular distribution of AnxA3 in the endocytic compartment of the cells suggests that the AnxA3 interaction with the vesicular trafficking involved in lipid droplet accumulation^{3,5,25,26} may represent a putative mechanism of lipid storage modulation in ccRCC cells.

Discussion

This study used primary cell cultures, established from ccRCC and normal cortex tissue samples, and human cell lines to investigate the involvement of AnxA3 isoforms in the lipid-laden clear cell morphology of ccRCC cells. Previous findings described AnxA3 to be a negative regulator of adipocyte differentiation in adipose tissue,⁷ suggesting the idea that AnxA3 may even modulate the storage of lipid droplets responsible for the adipocyte-like phenotype of ccRCC cells. Moreover, the gene expression profiling of ccRCC tissue revealed an adipogenic signature in this tumor.⁶

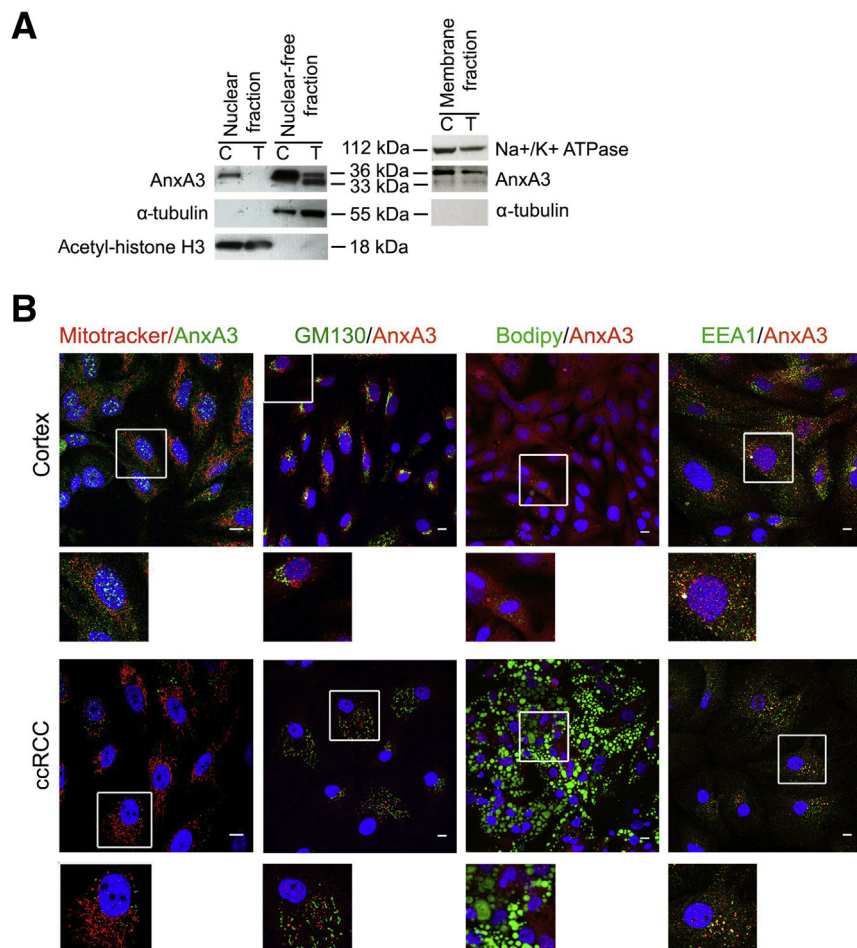


Figure 6 Subcellular distribution of annexin A3 (AnxA3) isoforms in normal cortex and clear cell renal cell carcinoma (ccRCC) primary cultures. **A:** Representative Western blot analysis of AnxA3 isoforms performed in nuclear, nuclear-free, and membrane fractions purified from matched cortex (C) and ccRCC (T) primary cultures. α -Tubulin, acetyl-histone H3, and Na⁺/K⁺ ATPase bands assessed the quality of subcellular fractionation. **B:** Immunofluorescence analysis of the AnxA3 protein distribution (in green or in red) in mitochondria (stained in red with Mitotracker), Golgi apparatus (stained in green with anti-130 kDa cis-Golgi matrix protein antibody), lipid droplets (stained in green with Bodipy), and early endosomes [stained in green with anti-early endosome antigen 1 (EEA1) antibody] of normal cortex and ccRCC cells. **Boxed areas** are shown at higher magnification below. Colocalization signal (in yellow) between AnxA3 and EEA1 is clear in the corresponding enlarged insets. Scale bars = 10 μ m (**B**). EEA1, early endosome antigen 1; GM130, golgin A2.

The ccRCC primary cultures in this study showed a grade-dependent expression of the lipid droplet marker PLIN2 and a prevalence of the 33-kDa versus the 36-kDa AnxA3 isoform, as previously described for the cultures obtained from different populations of patients.^{2,14} The quantitative ratio between the 36- and 33-kDa AnxA3 isoforms (36/33 ratio) was lower in lipid-laden low-grade ccRCC cultures with respect to high-grade cultures that showed a less abundant lipid droplet content, as also previously shown.² Moreover, the expression of PLIN2 in these ccRCC cultures negatively correlated with the 36/33 ratio, suggesting a molecular and functional link between the AnxA3 isoform pattern and lipid storage in ccRCC cells. *In silico* analysis of RNA-sequencing expression of a larger collection of ccRCC tissue samples from TCGA KIRC tissue data set confirmed these findings at transcript level and proved the reliability of our primary cell culture model. The 36/33 ratio inversely matched with PLIN2-positive lipid storage, even in ccRCC cell lines. The prevalence of the 36-versus the 33-kDa AnxA3 isoform characterized HK2 normal tubular and A498 ccRCC cell lines, both HIF1 α -negative, whereas HIF1 α -positive Caki1 ccRCC cells showed a prevalence of the 33- versus the 36-kDa isoform.

Notably, the up-regulation of the 36-kDa AnxA3 isoform has been previously described not only in normal cortex primary cultures but even in HIF1 α -negative RCC,¹⁴ and herein it was shown that PLIN2 expression was significantly higher and 36/33 ratio lower in HIF1 α -positive than in HIF1 α -negative ccRCC primary cultures. Therefore, the differential HIF1 α status described in Caki1 and A498 cells¹⁶ and in our ccRCC samples might justify their different AnxA3 isoform pattern and consequently their different lipid storage.

To better characterize the link between lipid storage and AnxA3 isoform expression in ccRCC cells, the effect was analyzed in our cell lines of the adipogenic medium described by Tun et al,⁶ used in this study as inducer of lipid storage. Herein, it was shown that 8 days of treatment with adipogenic medium affected the viability of HK2 proximal tubular cell line, suggesting a toxic effect of this medium in this cell type. Moreover, after 8 days of adipogenic treatment, a significant increment of lipid storage was observed only in Caki1 ccRCC cells. In these cells, the adipogenic treatment further reduced the already low expression of 36-kDa AnxA3. Watanabe et al⁷ used a medium with similar composition to induce the differentiation

of pre-adipocytes to adipocytes, observing a down-regulation of AnxA3 expression as well. Otherwise, 8 days of adipogenic treatment did not induce a significant increase of lipid storage and/or a down-regulation of 36-kDa AnxA3 in A498 ccRCC cells, which highly expressed this AnxA3 isoform. These data suggest that 36-kDa AnxA3 restricts the lipid storage induced by adipogenic treatment in ccRCC cells. To validate this hypothesis, the 36-kDa AnxA3 expression was specifically knocked down in A498 cells in the presence of adipogenic medium with a consequent decrease of the 36/33 ratio. A significant increment of PLIN2 expression was observed in A498 silenced cells with respect to control cells after 96 hours of adipogenic treatment. These data confirm that the 36-kDa AnxA3 and a high 36/33 ratio in ccRCC cells negatively modulate the response to adipogenic treatment and restrict lipid storage.

To investigate the mechanism responsible for the 36-kDa AnxA3-dependent modulation of lipid storage in ccRCC cells, the subcellular distribution of the AnxA3 isoforms was analyzed in normal cortex and ccRCC cells. The well-known phospholipid-binding ability of annexin family proteins²⁷ explains the presence of AnxA3 isoform protein bands not only in nuclear-free but also in purified membrane fractions of normal and ccRCC cells. The protein band of 36-kDa AnxA3, highly abundant in normal cortex cells, was detectable even in the nuclear fraction, where it may also be bound to the nuclear membrane. The lack in the N-terminal domain of the 33-kDa isoform of the tryptophan 5 residue that is involved in membrane binding^{14,28} may justify, in ccRCC cells, the absence of the 33-kDa band in the nuclear fraction and the prevalence of the 36- versus 33-kDa band in the purified membrane fraction. An AnxA3 signal was detected in cytoplasmic and membrane fractions even in hepatocellular carcinoma cells cultured in medium supplemented with recombinant AnxA3 protein. In these cells, the recombinant exogenous protein was internalized through a caveolin1-dependent endocytic pathway.¹⁰ The colocalization of AnxA3 and early endosome antigen 1 signals in our normal cortex and ccRCC primary culture cells proves that even endogenous AnxA3, in particular the 36-kDa isoform, which is well represented in membrane fractions, localized to the endocytic compartment. Otherwise, the endocytic uptake of exogenous lipids, through the caveolin1-dependent endocytosis, is involved in lipid storage during adipocyte differentiation,⁵ in which the caveolin1 expression is strongly up-regulated,²⁹ as well as in ccRCC cells.³⁰ In addition, an involvement of the endocytic uptake of neutral lipid-rich lipoproteins, mediated by the HIF1-dependent up-regulation of very-low-density lipoprotein receptor, has been also described in ccRCC cells.^{3,4,31} Therefore, the subcellular distribution of 36-kDa AnxA3 in the endocytic compartment suggests that it may negatively modulate lipid storage in ccRCC cells by interfering with the vesicular trafficking involved in lipid uptake and accumulation. In ccRCC cells that show low 36-kDa AnxA3

expression and 36/33 ratio, the reduced interference of AnxA3 with the endocytic-dependent uptake and storage of exogenous lipids might explain the abundant lipid accumulation.

The demonstration that 36-kDa AnxA3 negatively regulates lipid storage in ccRCC might have translational outcomes as well. In fact, lipid storage has been described to promote endoplasmic reticulum homeostasis and tumor cell survival in ccRCC.³² The delivery of exogenous 36-kDa AnxA3 protein and its internalization by caveolin1-dependent endocytosis into ccRCC cells might affect their survival by interfering with lipid uptake and storage.

Acknowledgments

We thank Francesca Sanguedolce (University of Foggia, Foggia, Italy) for providing hematoxylin-eosin staining tissue images; Silvia Coco (Milano-Bicocca University, Monza, Italy) for providing isobutylmethylxanthine; Ilaria Rivolta (Milano-Bicocca University, Monza, Italy) for providing 130 kDa cis-Golgi matrix protein and early endosome antigen 1 antibodies; and Andrew Smith for English proofreading of the manuscript.

Supplemental Data

Supplemental material for this article can be found at <http://doi.org/10.1016/j.ajpath.2020.08.008>.

References

1. Rezende RB, Drachenberg CB, Kumar D, Blanchaert R, Ord RA, Ioffe OB, Papadimitriou JC: Differential diagnosis between monomorphic clear cell adenocarcinoma of salivary glands and renal (clear) cell carcinoma. *Am J Surg Pathol* 1999, 23:1532–1538
2. Bianchi C, Meregalli C, Bombelli S, Di Stefano V, Salerno F, Torsello B, De Marco S, Bovo G, Cifola I, Mangano E, Battaglia C, Strada G, Lucarelli G, Weiss RH, Perego RA: The glucose and lipid metabolism reprogramming is grade-dependent in clear cell renal cell carcinoma primary cultures and is targetable to modulate cell viability and proliferation. *Oncotarget* 2017, 8:113502–113515
3. Perman Sundelin J, Stahlman M, Lundqvist A, Levin M, Parini P, Johansson ME, Boren J: Increased expression of the very low-density lipoprotein receptor mediates lipid accumulation in clear-cell renal cell carcinoma. *PLoS One* 2012, 7:e48694
4. Saito K, Arai E, Maekawa K, Ishikawa M, Fujimoto H, Taguchi R, Matsumoto K, Kanai Y, Saito Y: Lipidomic signatures and associated transcriptomic profiles of clear cell renal cell carcinoma. *Sci Rep* 2016, 6:28932
5. Le Lay S, Blouin CM, Hajdouch E, Dugail I: Filling up adipocytes with lipids: lessons from caveolin-1 deficiency. *Biochim Biophys Acta* 2009, 1791:514–518
6. Tun HW, Marlow LA, von Roemeling CA, Cooper SJ, Kreinest P, Wu K, Luxon BA, Sinha M, Anastasiadis PZ, Copland JA: Pathway signature and cellular differentiation in clear cell renal cell carcinoma. *PLoS One* 2010, 5:e10696
7. Watanabe T, Ito Y, Sato A, Hosono T, Niimi S, Ariga T, Seki T: Annexin A3 as a negative regulator of adipocyte differentiation. *J Biochem* 2012, 152:355–363
8. Gerke V, Creutz CE, Moss SE: Annexins: linking Ca²⁺ signaling to membrane dynamics. *Nat Rev Mol Cell Biol* 2005, 6:449–461

9. Park JE, Lee DH, Lee JA, Park SG, Kim NS, Park BC, Cho S: Annexin A3 is a potential angiogenic mediator. *Biochem Biophys Res Commun* 2005, 337:1283–1287
10. Tong M, Fung TM, Luk ST, Ng KY, Lee TK, Lin CH, Yam JW, Chan KW, Ng F, Zheng BJ, Yuan YF, Xie D, Lo CM, Man K, Guan XY, Ma S: AnxA3/JNK signaling promotes self-renewal and tumor growth, and its blockade provides a therapeutic target for hepatocellular carcinoma. *Stem Cell Rep* 2015, 5:45–59
11. Yan X, Yin J, Yao H, Mao N, Yang Y, Pan L: Increased expression of Annexin A3 is a mechanism of platinum resistance in ovarian cancer. *Cancer Res* 2010, 70:1616–1624
12. Yin J, Yan X, Yao X, Zhang Y, Shan Y, Mao N, Yang Y, Pan L: Secretion of Annexin A3 from ovarian cancer cells and its association with platinum resistance in ovarian cancer patients. *J Cell Mol Med* 2012, 16:337–348
13. Kollermann J, Schlomm T, Bang H, Schwall GP, von Eichel-Streiber C, Simon R, Schostak T, Huland H, Berg W, Sauter G, Klocker H, Schrattenholz F: Expression and prognostic relevance of Annexin A3 in prostate cancer. *Eur Urol* 2008, 54:1314–1323
14. Bianchi C, Bombelli S, Raimondo F, Torsello B, Angeloni V, Ferrero S, Di Stefano V, Chinello C, Cifola I, Invernizzi L, Brambilla P, Magni F, Pitto M, Zanetti G, Mocarelli P, Perego RA: Primary cell cultures from human renal cortex and renal cell carcinoma evidence a differential expression of two spliced isoforms of Annexin A3. *Am J Pathol* 2010, 176:1660–1670
15. Tang Z, Kang B, Li C, Chen T, Zhang Z: GEPIA2: an enhanced web server for large-scale expression profiling and interactive analysis. *Nucleic Acids Res* 2019, 47:556–560
16. Shinojima T, Oya M, Takayanagi A, Mizuno R, Shimizu N, Murai M: Renal cancer cells lacking hypoxia inducible factor (HIF)-1 α expression maintain vascular endothelial growth factor expression through HIF-2 α . *Carcinogenesis* 2007, 28:529–536
17. Bombelli S, Zipeto MA, Torsello B, Bovo G, Di Stefano V, Bugarin C, Zordan P, Viganò P, Cattoretti G, Strada G, Bianchi C, Perego RA: PKH high cells with clonal human nephrospheres provide a purified adult renal stem cell population. *Stem Cell Res* 2013, 11:1163–1177
18. Wettersten H, Hakimi AA, Morin D, Bianchi C, Johnstone ME, Donohoe DR, Trott JF, Abu Aboud O, Stirdivant S, Neri B, Wolfert R, Stewart B, Perego R, Weiss HR: Grade-dependent metabolic reprogramming in kidney cancer revealed by combined proteomics and metabolomics analysis. *Cancer Res* 2015, 75:2541–2552
19. Di Stefano V, Torsello B, Bianchi C, Cifola I, Mangano E, Bovo G, Cassina V, De Marco S, Corti R, Meregalli C, Bombelli S, Viganò P, Battaglia C, Strada G, Perego RA: Major action of endogenous lysyl oxidase in clear cell renal cell carcinoma progression and collagen stiffness revealed by primary cell cultures. *Am J Pathol* 2016, 186:2473–2485
20. Botto L, Beretta E, Bulbarelli A, Rivolta I, Lettieri B, Leone BE, Miserocchi G, Palestini P: Hypoxia-induced modifications in plasma membranes and lipid microdomains in A549 cells and primary human alveolar cells. *J Cell Biochem* 2008, 105:503–513
21. Raimondo F, Morosi L, Chinello C, Perego R, Bianchi C, Albo G, Ferrero S, Rocco F, Magni F, Pitto M: Protein profiling of microdomains purified from renal cell carcinoma and normal kidney tissue samples. *Mol Biosyst* 2012, 8:1007–1016
22. Raimondo F, Salemi C, Chinello C, Fumagalli D, Morosi L, Rocco F, Ferrero S, Perego R, Bianchi C, Sarto C, Pitto M, Brambilla P, Magni F: Proteomic analysis in clear cell renal cell carcinoma: identification of differentially expressed protein by 2-D DIGE. *Mol Biosyst* 2012, 8:1040–1051
23. Perego R, Corizzato M, Brambilla P, Ferrero S, Bianchi C, Fasoli E, Signorini S, Torsello B, Invernizzi L, Bombelli S, Angeloni V, Pitto M, Battaglia C, Proserpio V, Magni F, Galasso G, Mocarelli P: Concentration and microsatellite status of plasma DNA for monitoring patients with renal carcinoma. *Eur J Cancer* 2008, 44:1039–1047
24. Greenberg AS, Coleman RA, Kraemer FB, McManaman JL, Obin MS, Puri V, Yan QW, Miyoshi H, Mashek DG: The role of lipid droplets in metabolic disease in rodents and humans. *J Clin Invest* 2011, 121:2102–2110
25. Ouimet M, Franklin V, Mak E, liao X, Tabas I, Marcel YL: Autophagy regulates cholesterol efflux from macrophage foam cells via lysosomal acid lipase. *Cell Metab* 2011, 13:655–667
26. Wang J, Tan M, Ge J, Zhang P, Zhong J, Tao L, Wang Q, Tong X, Qiu J: Lysosomal acid lipase promotes cholesterol ester metabolism and drives clear cell renal cell carcinoma progression. *Cell Prolif* 2018, 51:e12452
27. Raynald P, Pollard HB: Annexins: the problem of assessing the biological role for a gene family of multifunctional calcium- and phospholipid-binding proteins. *Biochim Biophys Acta* 1994, 1197:63–93
28. Hofmann A, Raguene-Nicol C, Favier-Perron B, Mesonero J, Huber R, Russo-Marie F, Lewit-Bentley A: The Annexin A3 membrane interaction is modulated by an N-terminal tryptophan. *Biochemistry* 2000, 39:7712–7721
29. Scherer PE, Lisanti MP, Baldini G, Sargiacomo M, Mastick CC, Lodish HF: Induction of caveolin during adipogenesis and association of GLUT4 with caveolin-rich vesicles. *J Cell Biol* 1994, 127:1233–1243
30. Ruan HL, Li X, Yang HM, Song ZS, Tong JW, Cao Q, Wang KS, Xiao W, Xiao HB, Chen XY, Xu GH, Bao L, Ziong ZY, Yuan CF, Liu L, Qu Y, Hu WJ, Gao YY, Ru ZY, Chen K, Zhang XP: Enhanced expression of caveolin-1 possesses diagnostic and prognostic value and promotes cell migration, invasion and sunitinib resistance in the clear cell renal cell carcinoma. *Exp Cell Res* 2017, 358:269–278
31. Perman JC, Bostrom P, Lindbom M, Lidberg U, Stahlman M, Hagg D, Lindskog H, Scharin Tang M, Omerovic E, Mattsson Hulten L, Jeppsson A, Petursson P, Herlitz J, Olivecrona G, Strickland DK, Ekroos K, Olofsson SO, Boren J: The VLDL receptor promotes lipotoxicity and increases mortality in mice following an acute myocardial infarction. *J Clin Invest* 2011, 121:2625–2640
32. Qiu B, Ackerman D, Sanchez DJ, Li B, Ochocki JD, Grazioli A, Bobrovnikova-Marjon E, Diehl JA, Keith B, Simon MC: HIF2 α -dependent lipid storage promotes endoplasmic reticulum homeostasis in clear-cell renal cell carcinoma. *Cancer Discov* 2015, 5:652–667